High-precision atmospheric parameter and abundance determination of massive stars, and consequences for stellar and Galactic evolution

Journal of Physics: Conference Series **328** (2011) 012017 doi:10.1088/1742-6596/328/1/012017

High-precision atmospheric parameter and abundance determination of massive stars, and consequences for stellar and Galactic evolution

Maria-Fernanda Nieva[1,2], Norbert Przybilla[2] and Andreas Irrgang[2]

[1] Max-Planck-Institut für Astrophysik, Karl-Schwarzschild-Str. 1, D-85741 Garching, Germany
[2] Dr. Karl Remeis-Sternwarte & ECAP, Sternwartstr. 7, D-96049 Bamberg, Germany

E-mail: nieva@sternwarte.uni-erlangen.de

Abstract. The derivation of high precision/accuracy parameters and chemical abundances of massive stars is of utmost importance to the fields of stellar evolution and Galactic chemical evolution. We concentrate on the study of OB-type stars near the main sequence and their evolved progeny, the BA-type supergiants, covering masses of ∼6 to 25 solar masses and a range in effective temperature from ∼8000 to 35 000 K. The minimization of the main sources of systematic errors in the atmospheric model computation, the observed spectra and the quantitative spectral analysis play a critical role in the final results. Our self-consistent spectrum analysis technique employing a robust non-LTE line formation allows precise atmospheric parameters of massive stars to be derived, achieving 1σ-uncertainties as low as 1% in effective temperature and ∼0.05–0.10 dex in surface gravity. Consequences on the behaviour of the chemical elements carbon, nitrogen and oxygen are discussed here in the context of massive star evolution and Galactic chemical evolution, showing tight relations covered in previous work by too large statistical and systematic uncertainties. The spectral analysis of larger star samples, like from the upcoming Gaia-ESO survey, may benefit from these findings.

1. Introduction

Massive stars in the Galaxy are vastly outnumbered by lower-mass stars, like e.g. solar-type stars. Yet, massive stars are key drivers of the dynamics and evolution of the interstellar medium (ISM). As sources of ionizing radiation and momentum – via stellar winds and supernovae – they heat the ISM, initiate turbulence and contribute to the enrichment of the ISM with heavy elements. From the observer's perspective, massive stars are Galactic beacons throughout the UV to near-infrared wavelengths. They are observable not only nearby but out to large distances, tracing the star-forming regions within the spiral arms of the Milky Way. Massive stars are therefore key objects to understand the history and evolution of our Galaxy, and their study is of utmost relevance in the framework of the Gaia mission.

We concentrate here on the study of OB (late-O and early-B) main sequence stars and their progeny, the BA-type supergiants (BA-SGs) in order to trace their evolutionary history from the zero-age main sequence to the late stages of their life. The present sample of 64 stars covers a range in mass of ∼6 to 25 solar masses and a range in effective temperature from ∼8000 to 35 000 K. Highly accurate and precise stellar parameters and chemical abundances have been derived using robust spectral synthesis that accounts for deviations from the assumption of

local thermodynamic equilibrium (non-LTE) and a self-consistent spectral analysis that utilizes multiple ionization equilibria. While the method is superior to standard techniques – which employ photometric temperature indicators or the ionization equilibrium of only one element –, it is also more time consuming. We have therefore expanded our efforts to implement first a semi-automatic and now an almost fully-automatic analysis procedure in order to facilitate the study of larger star samples at similar accuracy and precision. As it will be shown here, the efforts to obtain high-quality results from high-resolution observations at high S/N-ratio are extremely valuable for the progress of several fields, like the evolution of the chemical elements in the Galaxy, the evolution of stars under different conditions and also the evolution of the ISM.

In the following, we briefly describe the star sample (Sect. 2), the codes used to compute the synthetic models in non-LTE (Sect. 3), as well as the self-consistent spectral analysis based in simultaneous fits of individual lines of hydrogen, helium and several metals (Sect. 4). Two main results of this work are presented, addressing the fields of stellar evolution (Sect. 5) and Galactic chemical evolution (Sect. 6). Finally, the conclusions are drawn in Sect. 7.

2. The star sample and observations

The star sample has been carefully chosen in order to avoid observationally induced systematic biases, see [1] for a discussion of selection criteria. The OB main sequence star sample contains 29 single, sharp-lined and chemically inconspicuous stars. The stars are located within a radius of 400 pc from the Sun. The BA supergiant sample is composed of 35 stars located at distances up to 4 kpc from the Sun. For the whole sample of OB dwarfs and BA-SGs observations have been collected with several high-resolution spectrographs, e.g. the Fiber-fed Extended Range Optical Spectrograph (FEROS) and the Fibre Optics Cassegrain Echelle Spectrograph (FOCES, at the 2.2m telescopes at La Silla and Calar Alto, respectively) and the FIbre-fed Echelle Spectrograph (FIES, at the Nordic Optical Telescope, La Palma) at high S/N-ratio (250 to 800). Details of the observations can be found in [1, 2] for the OB sample and in [3, 4, 5] for the BA-SG sample.

3. Spectrum synthesis in non-LTE

The non-LTE line-formation computations for the OB dwarfs follow the methodology discussed in detail in our previous studies for H and He [6], for C [7, 8], and for N, O, Ne, Mg, Si and Fe [9]. For the BA-SGs the methodology is described in [3], and references therein. In brief, a non-LTE approach is employed to solve the restricted non-LTE problem on the basis of prescribed LTE atmospheres. This technique provides an efficient way to compute realistic synthetic spectra in all cases where the atmospheric structure is close to LTE, like for the stars analysed here [6]. The computational efforts can thus be focused on robust non-LTE line-formation calculations.

3.1. Models and programs

The model atmospheres were computed with the ATLAS9 code [10] which assumes plane-parallel geometry, chemical homogeneity, and hydrostatic, radiative and local thermodynamic equilibrium. Line blanketing was realized here by means of opacity distribution functions (ODFs) from [11]. Solar abundances of [12] were adopted in all computations. The model atmospheres were held fixed in the non-LTE calculations. Non-LTE level populations and model spectra were obtained with recent versions of DETAIL [13] and SURFACE [14]. The coupled radiative transfer and statistical equilibrium equations were solved with DETAIL, employing an accelerated lambda iteration scheme of [15]. This allowed even complex ions to be treated in a realistic way. Synthetic spectra were calculated with SURFACE, using refined line-broadening theories. Continuous opacities due to hydrogen and helium were considered in non-LTE and line blocking was accounted for in LTE via Kurucz' ODFs. Updates of some of the published model atoms for non-LTE computations were carried out introducing improved oscillator strengths and collisional data from *ab-initio* computations, see [1, 3].

4. Spectral analysis

Our analysis method is based on the simultaneous reproduction of all spectroscopic indicators via an iterative line-fitting procedure aiming to derive atmospheric parameters and chemical abundances self-consistently. In contrast to common strategies in stellar spectroscopy, this analysis technique takes full advantage of the information encoded in the *line profiles* at different wavelength ranges simultaneously. Integrated quantities like equivalent widths W_λ are not used in this approach. The stellar parameters primarily derived here are the effective temperature $T_{\rm eff}$, surface gravity $\log g$, microturbulent velocity ξ, (radial-tangential) macroturbulent velocity ζ, projected rotational velocity $v \sin i$ and elemental abundances $\varepsilon(X) = \log(X/{\rm H}) + 12$.

4.1. Stellar parameter and abundance determination

Special emphasis was given to use multiple indicators in order to minimize the chance of the stellar atmospheric parameters and chemical abundance determination being biased by residual systematic errors. The following spectroscopic indicators were utilized in the analysis:

- $T_{\rm eff}$: all available hydrogen and helium lines, and multiple independent ionization equilibria; confirmation via spectral energy distributions (SEDs);
- $\log g$: wings of all available hydrogen lines and multiple ionization equilibria; for many of the OB dwarfs also confirmation via HIPPARCOS distances [16];
- ξ: several elements with spectral lines of different strength enforcing no correlation between $\varepsilon(X)$ and the strength of the lines (equivalent to $\varepsilon(X)$ being independent of W_λ);
- $v \sin i$ and ζ: metal line profiles;
- $\varepsilon(X)$: a comprehensive set of metal lines.

Usually in stellar analyses, once the stellar parameters are fixed one commences with the abundance determination, treating this as an essentially independent step. In our approach the abundance and stellar parameter determination are tightly related because of the use of ionization equilibria. In consequence, only few species are left to finalize the analysis. Another difference to typical literature studies is the large number of spectral lines evaluated by us per species (typically, ∼150 to 250 lines are analysed in total per star), see e.g. [1, 3], and the consistency achieved from the different ionization stages of the various elements. All the various improvements in observations, modelling and analysis methodology facilitated results at much higher accuracy to be achieved than possible in standard works, e.g. [17] to [29]. The high quality of the results could be retained over a large parameter space, spanning nearly 25 000 K in $T_{\rm eff}$ and ranging from close to the zero-age main sequence (ZAMS) to the late stages of evolution. Consequently, an excellent match of the computed and the observed spectra is achieved globally and in the details.

4.2. A semi-automatic analysis

We have computed a comprehensive grid of models (in total of the order ∼100 000 synthetic spectra) to perform the analysis. A powerful fitting routine for the semi-automatic comparison of observed and theoretical spectra, SPAS[1], provides the means to interpolate between model grid points for up to three parameters simultaneously and allows to apply instrumental, rotational and (radial-tangential) macrobroadening functions to the resulting theoretical profiles. Interactive work in some decisive steps on the analysis with SPAS paid off as much more accurate results could be obtained. Crucial was the selection of the appropriate spectroscopic indicators for the parameter determination which may vary from star to star upon availability of specific spectral lines (depending on stellar temperature, spectrum quality and the observed wavelength

[1] Spectrum Plotting and Analysing Suite, SPAS [30].

coverage). All spectral lines unsuited for analysis because of e.g. blends, low S/N, uncorrectable normalization problems, incomplete correction of cosmics, or known shortcomings in the modelling needed to be excluded. Also a verification and, possibly, correction of the automatic continuum normalization lead to a gain in precision. Every element was analysed independently and some interactive iterations for fine-tuning the parameter determination were needed in order to find a unique solution that reproduces all indicators simultaneously. This facilitated also to derive realistic uncertainties for the stellar parameters. The standard deviations around the average parameter values were adopted, as derived from the various independent spectral indicators. Likewise, uncertainties of elemental abundances were determined from the line-to-line scatter found from the analysis of the individual features. Finally, it was thus possible to derive a simultaneous, self-consistent solution for atmospheric parameters and chemical abundances, and also to quantify their statistical uncertainties. The novel approach [1] provides results meeting the same quality standard as our previous work, e.g. [8, 9].

4.3. A fully-automatic analysis

All pros and cons of the spectral analysis that have been learnt in the previous work have been recently encoded by one of us into an even more efficient and automatic procedure, allowing the whole previous analysis to be done even faster and at similar precision. The independent analyses per element and several interactive iterations until convergence of all parameters are hereby replaced by one simultaneous fit of the entire suitable spectrum (freed from features not included in our models such as missing lines, cosmics, telluric lines, reduction artifacts, among others). Interpolating in pre-calculated model grids, the technique applied is capable to sample the whole multi-parameter space spanned by atmospheric parameters and elemental abundances at the same time. For instance, line blends due to macroscopic effects (i.e. instrumental, rotational, and macroturbulent broadening) are thus implemented absolutely correct. With this method, atmospheric parameters and chemical abundances are objectively, simultaneously, and self-consistently constrained by exploiting all available spectroscopic indicators.

5. Implications for massive star evolution

The availability of atmospheric parameters and elemental abundances for larger star samples facilitates to stellar evolution models to be tested. Significant improvements in the accuracy and precision of the observational results are in particular valuable, as they allow such tests to be pursued in greater detail.

Energy production in massive stars is governed by the CNO cycles throughout most of their lifetime. The nuclear-processed material may reach their surface layers through rotational mixing already during their main-sequence phase [31] opening up a very powerful diagnostic to test models of stellar evolution. The changes of the surface abundances reflect the actions of the dominating CN-cycle initially, following a well-defined nuclear path.

Numerous studies of CNO abundances in massive stars of the Milky Way are available from the literature, mostly for early B-type stars close to the main sequence and for BA-SGs. We illustrate the results of several key publications in the N/O–N/C diagrams of Fig. 1. Some of the more recent studies [17, 18, 19] are based on non-LTE model atmospheres, while the bulk of the data were obtained from non-LTE line-formation computations on LTE model atmospheres – which is equivalent to the full non-LTE approach in the cases under consideration [6].

The main-sequence stars show overall a wide range of N/O–N/C combinations, with the deviations from the predictions increasing in the supergiants. This picture is difficult to be interpreted – even more so if only one of the elements (like nitrogen) is considered. Moreover, several observational data points pose a challenge for the evolution models. On the other hand, the abundance uncertainties are very large, with a typical statistical 1σ-error in abundance per element of about a factor $\sim$2, while systematic uncertainties are often largely underestimated

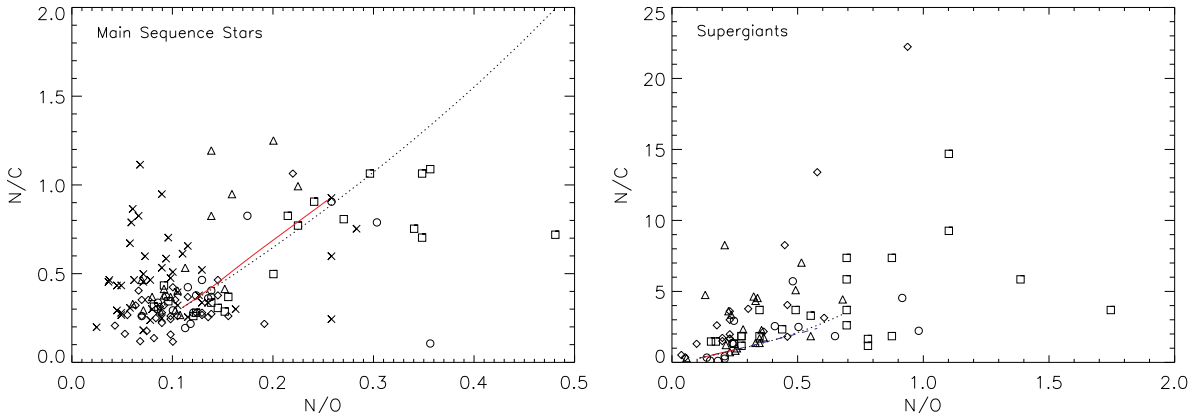

Figure 1. Observational constraints on the mixing of CNO-burning products in massive stars from non-LTE analyses in the literature. Mass ratios N/C over N/O are displayed. Left-hand panel: main-sequence stars. Circles: [20]; triangles: [21]; diamonds: [22, 23, 24, 25]; squares: [26]; crosses: [19]. Right-hand panel: BA-type supergiants. Triangles: [27], [28]; circles: [29]; squares: [17]; diamonds: [18]. Error bars can be larger than the plotting range. The lines represent predictions from evolution calculations, for a rotating 15 $M_{\odot}$ star with $v_{\rm rot}^{\rm ini} = 300\,{\rm km\,s^{-1}}$ until the end of the main sequence: solid red line, until the end of He burning: dashed blue line [32], and for a star of the same parameters that in addition takes the interaction of rotation and a magnetic dynamo into account [33], until the end of the MS: dotted line, respectively. The predicted trends are similar for the entire mass range under investigation.

(for a discussion of this see [34]) or even unaccounted for. The error bars in Fig. 1 are larger than the entire plotting range in many cases. In consequence, no *definite* conclusions can be drawn on the quality of the stellar evolution models from these data.

The behaviour of CNO abundances, previously presented for a sub-sample of 20 stars in [35], is now shown for the whole star sample of 64 stars in Fig. 2. In contrast to the literature values (Fig. 1), a clear and tight trend is found, confirming the predicted locus of N/O–N/C abundance ratios. Most of our main-sequence objects cluster around the pristine Cosmic Abundance Standard (CAS) values [1], i.e. they are unmixed, while about 1/3 of the stars show a mixing signature of varying magnitude, following the predicted nuclear path with $\mathrm{d(N/C)/d(N/O)} = 4.6$ (for initial CAS abundances) tightly. Stellar evolution models based e.g. on the solar values by [36] would predict a different nuclear path (with slope $\sim$3.0).

However, as already indicated above, the models of [32] for rotating stars with mass loss evolving towards the red supergiant stage (solid line in Fig. 2) predict mixing that is too low (see [35]), in particular for most of the supergiants. Five reasons may provide an explanation.

I) Higher than average rotation velocities in the progenitor stars of these supergiants on the main sequence may reconcile the situation for some objects.
II) Evolution models for rotating stars that also account for the interaction of rotation and a magnetic dynamo [33] predict enhanced mixing signatures of the amount required (dotted line).
III) Some stars may have evolved in a close binary, which can also lead to enhanced mixing associated with mass transfer.
IV) Some objects may have been siblings to τ Sco on the main sequence, climbing up the N/O–N/C relation even further in their further evolution.
V) Supergiants may already have evolved through the red supergiant phase (e.g., on a blue loop) to expose first dredge-up abundance ratios, which could quantitatively also explain the observations (dashed line).

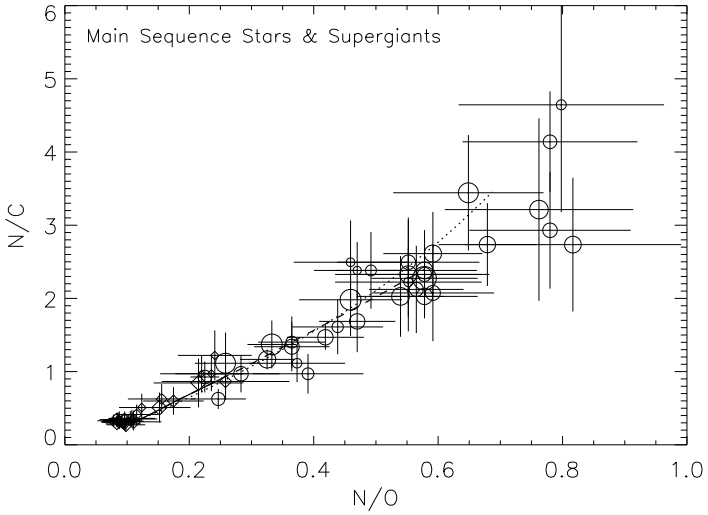

Figure 2. N/C vs. N/O abundance ratios (by mass) of our non-LTE analysis for the sample of 64 stars. B-type main-sequence stars are displayed as diamonds, BA-type supergiants as circles. The symbol size encodes the stellar mass and error bars give 1σ-uncertainties. The different lines describe evolutionary model predictions for $15\,M_{\odot}$ stars identical to those in Fig. 1.

6. Implications for Galactic chemical evolution

Nucleosynthesis in successive generations of stars has enriched the cosmic matter with heavy elements ever since the first Population III stars were born. Studies of various objects like Galactic stars, planetary nebulae and H II regions allow the cosmic enrichment history to be traced and the specific production sites of individual elements to be constrained. The Cosmic Abundance Standard (CAS), derived from our sample of unmixed B-stars, provides valuable input for the comparison of models with observations, as it marks the *present-day endpoint of Galactochemical evolution*, in particular for a typical spiral galaxy like the Milky Way. Here, we concentrate on the role of the CAS values in the context of the Galactic evolution of the light elements CNO as traced by stellar analyses, see Fig. 3.

Our achievements in improving the precision and accuracy of the B-star analyses over previously published work, relative to the trends in the evolution of the CNO abundances as derived from solar-type stars, become obvious in the comparison of the left- and right-hand panels of Fig. 3. While the enormous scatter in the B-star abundances was difficult to be reconciled with the data from solar-type stars in the past, our data for the B-stars indicate a high degree of chemical homogeneity, at absolute abundance values that may differ from the solar standard.

While the investigations of the cosmic chemical evolution are currently focusing on the early phases at low metallicity, an accurate knowledge of the present-day endpoint of the evolution is nonetheless essential. The reason for this is that the interpretation of the data is based on comparisons with Galactic chemical evolution models, which have to (but not always do) match the present-day composition as a boundary condition. It is therefore important for the entire modelling which reference values are used, solar or CAS abundances. In particular the differences in the C/O ratio are appreciable, also with respect to the majority of nearby solar-type stars, amounting to almost 50%. Taken at face value, this difference indicates that the C/O enrichment of the interstellar medium in the present-day solar neighborhood occurred slower than at the

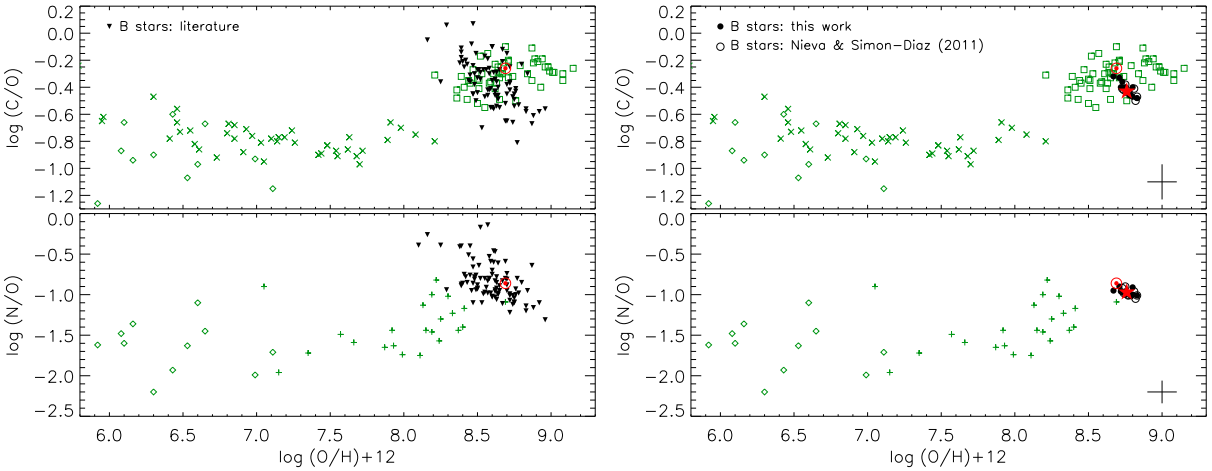

Figure 3. Observational constraints on the chemical evolution of Galactic CNO abundances: abundance ratios log (C/O) and log (N/O) vs. O abundance. *Left-hand panels*: black triangles: early B-stars from the literature, like in Fig. 1, except for [19]. Data for low-mass stars are displayed as green symbols – squares: solar-type dwarfs [37]; crosses: solar-type dwarfs and subgiants [38]; diamonds: unmixed cool giants [39]; plus signs: unevolved solar-type stars [40]. Solar abundance ratios of [36] are also indicated ($\odot$). *Right-hand panels*: black dots: unmixed B-type stars from the present work, black circles: unmixed stars from [2]. Data from the literature like in the left-hand panels. The Cosmic Abundance Standard is also indicated (red star). Error bars typical for individual stars in the present study are shown.

Sun's place of birth.

Note that the Sun may be viewed as an extreme but still compatible case in terms of the distribution of the stars from the present sample in the log O–log C/O diagram, but the absolute values for the carbon abundance differ significantly. The solar and CAS data on N/O are rather compatible on the other hand. A systematic investigation of nitrogen abundances in high-metallicity solar-type stars would be desirable for further comparisons.

Overall, it is astonishing how different and at the same time how similar the young and old star populations in the solar neighborhood are. It is for the first time that this is elaborated, as the lack of high precision and accuracy in many previous studies of early B-type stars prevented any meaningful conclusions to be drawn.

7. Conclusions

Over the past few years, we have made great efforts to reduce uncertainties in quantitative spectral analyses of OB-type stars near the main sequence and their evolved progeny, BA-type supergiants. Self-consistent analyses that bring all spectroscopic indicators – Balmer, helium lines and metal ionization equilibria – into match simultaneously yield drastically reduced systematic errors in the determination of atmospheric parameters and chemical abundances. More recent work focused on the development of a fully-automatic fitting routine for the analysis of much larger samples of stars than feasible at present. We are confident that future studies of early-type stars, like within the ESO-Gaia survey, will largely benefit from these developments.

This leap in the accuracy and precision of early-type star analyses has already produced some exciting results. We gave concrete examples on the behaviour of the light elements CNO in the context of stellar and Galactic chemical evolution, which will stimulate further investigations by theorists that will give meaningful answers to several of today's fundamental astrophysical questions.

References

[1] Nieva M F and Przybilla N *A&A*, submitted
[2] Nieva M F and Simón-Díaz S 2011 *A&A* **532** 2
[3] Przybilla N, Butler K, Becker S R and Kudritzki R P 2006 *A&A* **445** 1099
[4] Schiller F and Przybilla N 2008 *A&A* **479** 849
[5] Firnstein M 2010 *Ph.D. Thesis* (Univ. Erlangen-Nuremberg)
[6] Nieva M F and Przybilla N 2007 *A&A* **467** 295
[7] Nieva M F and Przybilla N 2006 *ApJ* **639** L39
[8] Nieva M F and Przybilla N 2008 *A&A* **481** 199
[9] Przybilla N, Nieva M F and Butler K 2008 *ApJ* **688** L103
[10] Kurucz R L 1993b *CD-ROM No. 13* (Cambridge, Mass.: SAO)
[11] Kurucz R L 1993a *CD-ROM No. 2–12* (Cambridge, Mass.: SAO)
[12] Grevesse N and Sauval A J 1998 *Space Sci. Rev.* **85** 161
[13] Giddings J R 1981 *Ph.D. Thesis* (Univ. London)
[14] Butler K and Giddings J R 1985 in *Newsletter of Analysis of Astronomical Spectra, No. 9* (Univ. London)
[15] Rybicki G B and Hummer D G 1991 *A&A* **245** 171
[16] van Leeuwen F 2007 *Hipparcos, the new reduction of the raw data* (Dordrecht: Springer)
[17] Crowther P A, Lennon D J and Walborn N R 2006 *A&A* **446** 279
[18] Searle S C, Prinja R K, Massa D and Ryans R 2008 *A&A* **481** 777
[19] Hunter I *et al.* 2009 *A&A* **496** 841
[20] Kilian J 1992 *A&A* **262** 17
[21] Gies D R and Lambert D L 1992 *ApJ* **387** 673
[22] Cunha K and Lambert D L 1994 *ApJ* **426** 170
[23] Daflon S, Cunha K and Becker S R 1999 *ApJ* **522** 950
[24] Daflon S, Cunha K, Becker S R and Smith V V 2001a *ApJ* **552** 309
[25] Daflon S, Cunha K, Butler K and Smith V V 2001b *ApJ* **563** 325
[26] Morel T, Hubrig S and Briquet M 2008 *A&A* **481** 453
[27] Venn K A 1995 *ApJ* **449** 839
[28] Venn K A and Przybilla N 2003 in *ASP Conf. Ser.* **304** 20
[29] Takeda Y 2000 *PASJ* **52** 113
[30] Hirsch H 2009 *Ph.D. Thesis* (Univ. Erlangen-Nuremberg)
[31] Maeder A and Meynet G 2000 *ARA&A* **38** 143
[32] Meynet G and Maeder A 2003 *A&A* **404** 975
[33] Maeder A and Meynet G 2005 *A&A* **440** 1041
[34] Nieva M F and Przybilla N 2010 *ASP Conf. Ser.* **425** 146
[35] Przybilla N, Firnstein M, Nieva M F, Meynet G and Maeder A 2010 *A&A* **517** A38
[36] Asplund M, Grevesse N, Sauval A J and Scott P 2009 *ARA&A* **47** 481
[37] Gustafsson B, Karlsson T, Olsson E, Edvardsson B and Ryde N 1999 *A&A* **342** 426
[38] Fabbian D, Nissen P E, Asplund M, Pettini M and Akerman C 2009 *A&A* **500** 1143
[39] Spite M *et al.* 2005 *A&A* **430** 655
[40] Israelian G, Ecuvillon A, Rebolo R, García-López R, Bonifacio P and Molaro P 2004 *A&A* **421** 649